THE CONSTITUTION AND STRUCTURE OF MANGANESE-GALLIUM ALLOYS

By H. G. Meissner, K. Schubert and T. R. Anantharaman,* F.A.Sc.

(*Max-Planck-Institut fuer Metallforschung, Stuttgart, West Germany*)

Received October 24, 1964

1. Introduction

The work described in this paper forms part of a systematic investigation of the constitution of alloys of gallium with the transition metals.

The manganese-gallium system is of considerable interest in view of the existence of four structural modifications of manganese and the wide difference between the melting points of the two metals. The only previous work on this system is due to Zwicker (1951) who studied the influence of gallium on the three structural changes in solid manganese. Two intermediate phases, hexagonal close-packed and tetragonal respectively, were detected and later incorported in a very tentative sketch (Thiele and Zwicker, 1958) of the manganese-rich portion of the binary system. The present work, which has already been reported partially and briefly (Schubert *et al.*, 1960, 1962), covers the whole manganese-gallium system and is based essentially on thermal analysis and X-ray studies.

2. Experimental Procedure

Manganese-gallium alloys of thirty-five different chosen compositions were prepared from electrolytic manganese (99·8% pure) and high-grade gallium (99·99% pure). Alloys containing 5 to 50 atomic % gallium were melted in sintered corundum crucibles under argon and cooled in the electric furnace itself. Alloys richer in gallium were melted in evacuated and sealed quartz tubes in a suitable gas flame and quenched in water. The quartz tubes were not attacked in any way at these alloy compositions. In both methods of alloy preparation, there was only a negligible change in weight due to the melting process.

The alloys were homogenized at appropriate maximum temperatures in sealed quartz tubes under argon at pressures of about 1·5 atmospheres

* Now at Department of Metallurgy, Banaras Hindu University, Varanasi-5, India.

at the respective temperatures. After quenching in water, powder specimens of the alloys were prepared for X-ray examination by filing or grinding with a pestle. These were heat-treated in evacuated and sealed quartz tubes at appropriate temperatures and finally quenched in water. The powder photographs were invariably recorded with monochromatic CuK_α X-radiation in a Guinier camera (De Wolff-Nonius model).

The thermal analysis was conducted in an electric furnace with alloys weighing about 1·5 gm. each and kept in sintered corundum crucibles in an argon atmosphere. The furnace was heated and cooled through current fed from a transformer and controlled by an electric motor. The differential thermal analysis curves were registered on photographic paper through two mirror galvanometers and had an accuracy of not less than $\pm$ 10° C.

It has to be mentioned here that alloys with more than 65 atomic % gallium suffered a considerable increase in volume on cooling due to the formation of the $MnGa_4$ intermetallic phase and often collapsed into porous pieces or powdery material. Pressing into compacts was resorted to, wherever necessary.

3. Experimental Results

Text-Figures 1 to 4, Pl. XVI, Fig. 1 and Tables I to VII contain the results of the present investigations. Zwicker's findings (1951) concerning the influence of gallium content on the stability of the different allotropic modifications of manganese have been generally confirmed in this work.

The face-centred cubic γ-Mn phase, which is capable of dissolving more than 25 atomic % gallium at about 1000° C., is formed at 1180° C. by a peritectic reaction and decomposes eutectoidally at about 650° C. (Text-Fig. 1). It can be quenched to room temperature from 700° C. in alloys containing more than 20 atomic % gallium. The metastable tetragonal modification of this phase [γ-Mn (t), $a = 3{\cdot}79$ Å, $c/a = 0{\cdot}96_8$] is obtained on quenching alloys with 10 to 20 atomic % gallium from 800 to 1000° C. and coexists with the cubic γ-Mn phase in the $Mn_{80}Ga_{20}$ alloy (Table I). All γ-phase alloys are hard and plastic, but become brittle on transformation to the β-Mn phase. The alloy $Mn_{75}Ga_{25}$ is somewhat ductile after annealing at 600° C., but this is considered to be due to the presence of the ϵ phase. The $\beta \rightarrow \alpha$ transformation was not studied in detail in the present work. The alloys containing 20 and 25 atomic % gallium displayed continuous thermal analysis effects starting at 1110 and 1035° C. and ending at 1085 and 1027° C. respectively. The cause of these effects is not clear.

The ferromagnetic, hexagonal close-packed ϵ phase ($a = 2{\cdot}67_8$ Å, $c/a = 1{\cdot}62_0$), to which the formula $\sim Mn_2Ga$ (h) can be ascribed, can be quenched from 850° C. as a homogeneous phase in the composition range $Mn_{70}Ga_{30}$ to $Mn_{65}Ga_{35}$ in powder specimens. This phase is formed peritectically at about 995° C. and seems to decompose eutectoidally at about 530° C.

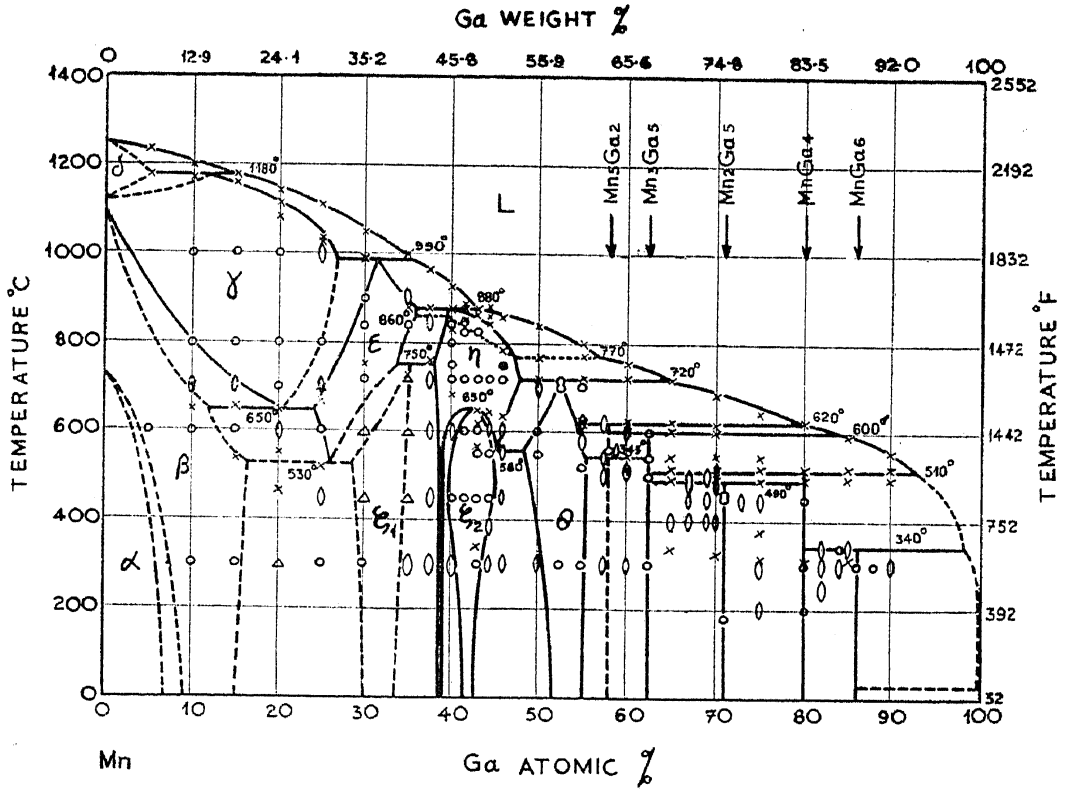

TEXT-FIG. 1. The manganese-gallium equilibrium diagram.

(Full lines—settled data; dotted lines—doubtful and needs confirmation; ×—thermal analysis arrests; o—single phase; 0—two-phase; Δ—uncertain equilibrium.)

(Text-Fig. 1). The equilibrium below 750° C., where the ϵ phase combines with the η phase peritectoidally to form the ζ_1 phase, is difficult to attain and hence the temperature of the eutectoidal reaction near 530° C. needs further experimental confirmation. In this composition range the filings obtained from the cast alloy, and from the regulus after annealing at 300° C., displayed in the powder patterns very broad 111- and 200-reflections of the γ phase characterized by a heavy stacking fault density. Only after long annealing of the powder followed by quenching in water could the patterns due to the ϵ and ζ_1 phases be obtained.

The ferromagnetic, face-centred tetragonal ζ_1 phase ($a = 3{\cdot}89_8$ Å, $c/a = 0{\cdot}92_0$), whose composition range also corresponds to the formula

~Mn_2Ga (r), forms peritectoidally at about 750° C. with 36 atomic % gallium (Text-Fig. 1). The existence of a peritectoidal reaction is generally ascertained only with difficulty in view of its slow nature, but the thermal analysis effects and the slow approach to equilibrium below 750° C. of alloys in this region of the phase diagram leave no room for any doubt concerning this particular reaction.

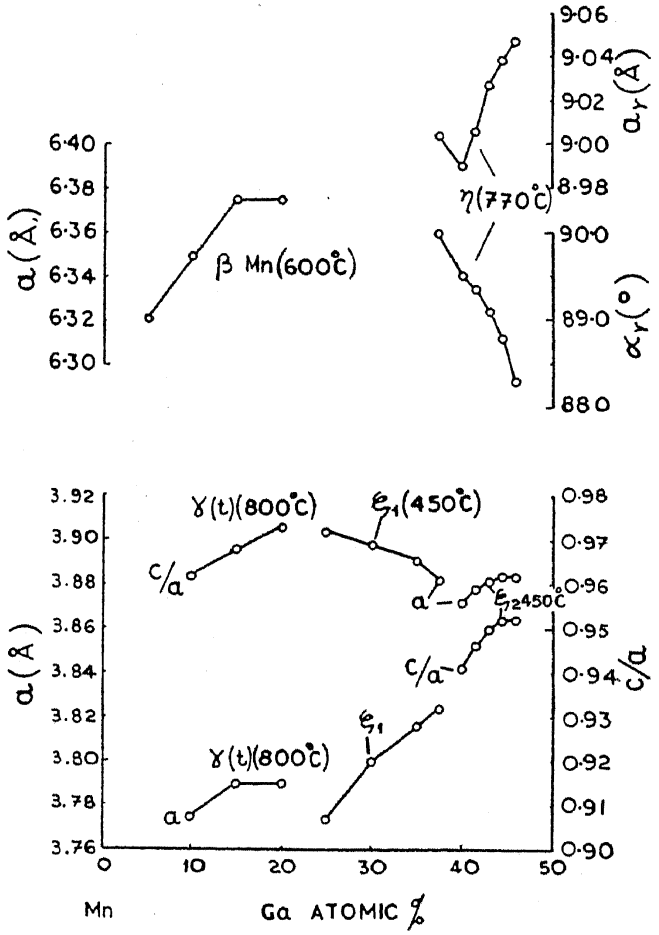

TEXT-FIG. 2. Variation of lattice parameters of some phases of the manganese-gallium system.

The ϵ and ζ_1 phases are both in equilibrium on the gallium-rich side with the rhombohedral η phase ($a = 8{\cdot}99$–$9{\cdot}05$ Å, $\alpha = 90{\cdot}0$–$88{\cdot}3°$), which is formed at 880° C. by a peritectic reaction (Text-Fig. 1). Alloy powders containing 39 to 47 atomic % gallium and quenched in water after annealing at 720° C. yield exclusively reflections of the η phase which can be indexed on hexagonal as well as rhombohedral axes (Table II). On the manganese-rich side the hexagonal axial ratio corresponds to the ideal cubic value of $c/a = 1{\cdot}225$. The B2 substructure appears with superstructure lines indexed with a three-fold

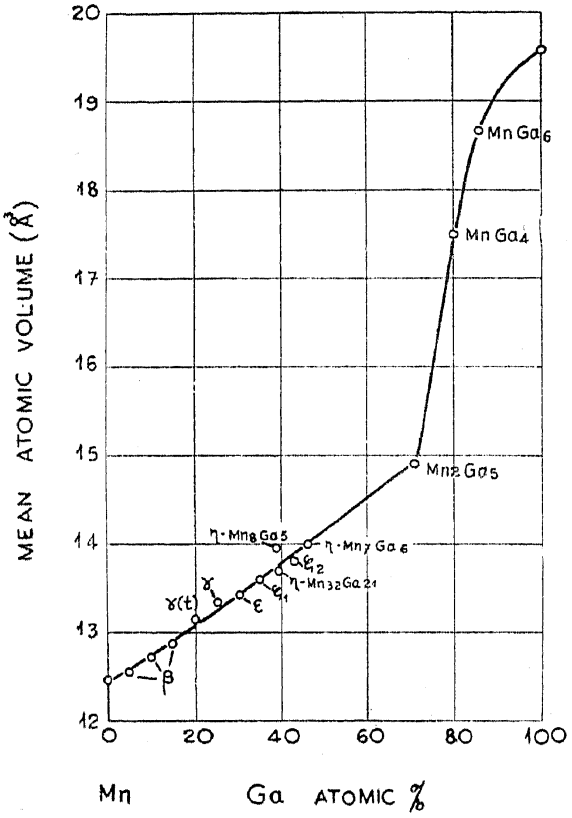

TEXT-FIG. 3

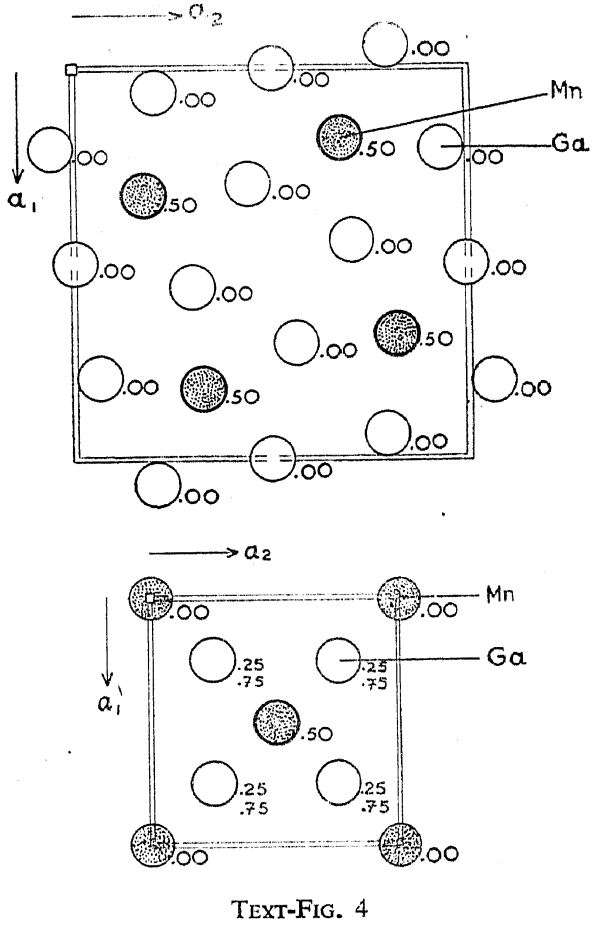

TEXT-FIG. 4

TEXT-FIG. 3. Mean atomic volumes of manganese-gallium alloys.

TEXT-FIG. 4. Structures of Mn_2Ga_5 and $MnGa_4$.

[*Above*, Mn_2Ga_5—D_{4h}^5-P4/mbm; $a = 8{\cdot}80_3$ Å; $c = 2{\cdot}69_4$ Å; 4 Mn (*h*) $x = 0, 180$; 8 Ga (*i*) $x = 0{\cdot}063$, $y = 0{\cdot}204$; 2 Ga (*d*).

Below, $MnGa_4$—0^5-I432; $a = 5{\cdot}59_1$ Å; 2 Mn (*a*); 8 Ga (*c*).]

cubic *a*-axis. But the structure is not of the body-centred cubic γ-brass type, as the reflection $(221)_{cubic} = (311)/(303)/(105)_{hexagonal}$ is recorded. The η phase gradually changes over with increasing gallium content to the already reported Cr_5Al_8 type (Schubert *et al.*, 1960) which is closely related to the γ-brass type. First determined by Bradley and Lu (1937), the Cr_5Al_8 structure can be considered as a rhombohedrally distorted γ-brass structure. Table II contains data on the powder reflections of the $Mn_{54}Ga_{46}$ alloy indexed on the basis of hexagonal as well as rhombohedral axes, the latter indices fulfilling the centering requirement: "*hkl* only with $h + k + l = 2n$". In view of the incomplete nature of the earlier data on Cr_5Al_8, we have also included in Table II our own results for that phase.

As the η phase proves to be homogeneous on the basis of X-ray data from powders quenched from 720° C. in the composition range Mn_8Ga_5 to Mn_7Ga_6, it is possible to differentiate between the quasi-cubic, non-body-centred and the rhombohedral, body-centred extremes of its structure. The powder photographs indicate clearly, however, that the rhombohedral distortion sets in gradually with increasing gallium content in a single-phase region. The hexagonal axial ratio increases from 1·225 to 1·28, while the rhombohedral angle decreases from 90° to 88·3° in this composition range. At lower temperatures, the quasi-cubic, manganese-rich phase is the only stable phase. In the composition range of 41–45 atomic % gallium the phase η transforms at about 650° C. on cooling to the ferromagnetic, face-centred tetragonal ζ_2 phase, which corresponds to the ζ_1 phase appearing at lower gallium contents, but displays the higher axial ratio of $0{\cdot}94_1$ to $0{\cdot}95_2$. On the other hand, the rhombohedral, gallium-rich η phase with 45·5 atomic % gallium undergoes at about 560° C. a eutectoidal reaction leading to the ζ_2 and θ phases on cooling (Text-Fig. 1). The hard and brittle η phase is thus transformed to a very ductile alloy on slow cooling. The weak thermal analysis effects observed in the range of 860°–770° C. in alloys containing 40 to 52·5 atomic % gallium (Table I) suggest the existence of a high-temperature phase that cannot be quenched to room temperature, in analogy with the related manganese-aluminium system (Koester and Wachtel, 1960).

The θ and Mn_5Ga_7 phases are formed peritectically at 720° and 620° C. respectively. Their powder photographs yield numerous reflections (Pl. XVI, Fig. 1) that point to their having closely related structures of the distorted γ-brass type. From a weak thermal analysis effect obtained in the alloys to $Mn_{25}Ga_{75}$ between 547° and 543° C., and from slight differences in the $Mn_{40}Ga_{60}$ diffraction pattern of Mn_5Ga_7 (not listed in Pl. XVI, Fig. 1 and Table I) we conclude that Mn_5Ga_7 undergoes a phase transformation at about 545° C. The Mn_3Ga_5 phase is also formed peritectically at about 600° C., but its equally complex powder photograph (Pl. XVI, Fig. 1) has similarities more to that of the η phase.

The ferromagnetic, tetragonal Mn_2Ga_5 phase ($a = 8{\cdot}80_3$ Å, $c/a = 0{\cdot}30_6$) is formed by a peritectoidal reaction between the Mn_3Ga_5 and $MnGa_4$ phases at about 490° C. The thermal analysis results and the data of numerous powder photographs of alloys in this composition range annealed between 450° and 520° C. clearly point to the existence of this slow, solid-state reaction. The data in Table III confirm the formula Mn_2Ga_5 and the structure type of Mn_2Hg_5 by comparison with the available data for Mn_2Hg_5 (de Wet, 1961).

TABLE I

Data on the constitution of manganese-gallium alloys

No.	Composition atomic %		Thermal analysis arrests (° C.)	Heat treatment				X-ray analysis results
				Regulus		Powder		
	Mn	Ga		Temperature (° C.)	Time	Temperature (° C.)	Time	
1	95	5	1235; 1180	as-cast		600	1 hr.	β-Mn
2	90	10	1200; 1170	as-cast				β-Mn
			700; 650	1000	5 hrs.	1000	5 min.	γ-Mn (*t*)
						800	30 min.	γ-Mn (*t*)
						700	1 hr.	β-Mn + γ-Mn (*t*)
				600	30 hrs.	600	2 hrs.	β-Mn
						300	200 hrs.	β-Mn
3	85	15	1180; 1160	as-cast				γ-Mn
			655; 540	1000	5 hrs.	1000	5 min.	γ-Mn (*t*)
						800	30 min.	γ-Mn (*t*)
						700	1 hr.	β-Mn + γ-Mn (*t*)
				600	30 hrs.	600	2 hrs.	β-Mn
						300	200 hrs.	β-Mn
4	80	20	1145; 1115	as-cast				γ-Mn
			1085; 650	1000	5 hrs.	1000	5 min.	γ-Mn (*t*) + γ
			(555); (470)			800	30 min.	γ-Mn (*t*) + γ
						700	1 hr.	γ-Mn (*t*) + γ
				600	30 hrs.	600	2 hrs.	β-Mn + ε
						300	200 hrs.	β-Mn + ζ_1 (+ ε)

5	75	25	1110; 1035	as-cast					γ
			1027; 700	1000	5 hrs.	1000	5 min.	$\gamma + \epsilon$
			670; 520			800	30 min.	γ
						700	1 hr.	$\gamma + \epsilon$
				600	30 hrs.	600	2 hrs.	ϵ
						450	10 hrs.	β-Mn $+ \epsilon$
				300	200 hrs.	..		γ
						300	8 hrs.	ζ_1
6	70	30	1050; 990	as-cast					$\gamma + \epsilon + \eta$
			755	840	12 hrs.				$\gamma + \epsilon$
						900	10 min.	ϵ
						840	15 min.	ϵ
				720	50 hrs.	1000	5 min.	ϵ
							(incipient melting)	
						720	3 hrs.	ϵ
						600	6 hrs.	ϵ
						450	5 hrs.	$\epsilon + \xi_1$
						300	100 hrs.	$\epsilon + \xi_1$
				300	200 hrs.			γ
						300	8 hrs.	ζ_1
7	65	35	1000; 880	as-cast					$\epsilon + \eta$
			730	840	12 hrs.				$\epsilon + \eta$
						900	10 min.	$\epsilon + \eta$
						840	15 min.	ϵ
				720	50 hrs.	720	3 hrs.	$\epsilon + \zeta_1 + \eta$
						600	6 hrs.	$\epsilon + \zeta_1$
						450	5 hrs.	$\epsilon + \zeta_1$
						300	100 hrs.	$\epsilon + \zeta_1$
				800	20 hrs.			
				+300	200 hrs.			γ
						300	8 hrs.	$\zeta_1 + \eta$

TABLE I (*Contd.*)

No.	Composition atomic %		Thermal analysis arrests (° C.)	Heat treatment				X-ray analysis results
				Regulus		Powder		
	M	Ga		Temperature (° C.)	Time	Temperature (° C.)	Time	
8	62·5	37·5	965; 880 760	850	50 hrs.	850	30 min.	$\epsilon + \eta$
						720	1 hr.	$\zeta_1 + \eta$
						450	5 hrs.	$\zeta_1 + \eta$
				720	50 hrs.	720	1 hr.	$\zeta_1 + \eta$
				300	8 days			$\zeta_1 + \eta$
						300	8 hrs.	$\zeta_1 + \eta$
9	60	40	930; 880 (828); (685)	840	12 hrs.	900	10 min.	$\epsilon + \eta$
							(incipient melting)	
						840	15 min.	η
				720	50 hrs.	720	3 hrs.	η
						600	2 hrs.	$\eta + \zeta_2$
						450	5 hrs.	ζ_2
						300	100 hrs.	$\eta + \zeta_2$
10	58·5	41·5	890; 880 855	850	20 hrs.	850	30 min.	η
				720	50 hrs.	720	3 hrs.	η
						600	2 hrs.	ζ_2
						450	5 hrs.	ζ_2
11	57	43	880; 865 650; 620 565; 340	850	15 hrs.	850	30 min.	η
					(incipient melting)			
						825	30 min.	η
				720	50 hrs.	720	3 hrs.	η
						600	2 hrs.	ζ_2
						450	5 hrs.	ζ_2
				550	30 hrs.			ζ_2
						300	30 hrs.	ζ_2

12	55·5	44·5	885; (860) (845); (645)	850	20 hrs.	850	30 min.	η
					(incipient melting)			
						825	30 min.	η
							(incipient melting)	
				720	50 hrs.	720	3 hrs.	η
						600	2 hrs.	$\eta + \zeta_2$
						550	5 hrs.	ζ_2
						450	5 hrs.	ζ_2
				550	30 hrs.	380	30 hrs.	$\zeta_2 + \theta$
						300	30 hrs.	$\zeta_2 + \theta$
13	54	46	860; 785	as-cast				η
			750; 635	840	12 hrs.	840	15 min.	η
					(incipient melting)			
				720	50 hrs.	800	30 min	η
							(incipient melting)	
						750	50 min.	η
						720	3 hrs.	η
						600	2 hrs.	$\eta + \theta$
						550	5 hrs.	$\zeta_2 + \theta$
						300	100 hrs.	$\zeta_2 + \theta$
14	50	50	840; 771	as-cast				$\eta + \theta$
			720	800	200 hrs.			η
					(incipient melting)			
				700	60 hrs.			$\eta + \theta$
						750	90 min.	η
							(incipient melting)	
						720	3 hrs.	η
							(incipient melting)	
						600	2 hrs.	θ
						550	5 hrs.	θ
						300	20 hrs.	$\zeta_2 + \theta$
15	47·5	52·5		700	60 hrs.	750	90 min.	η
							(incipient melting)	
						720	3 hrs.	θ
						300	20 hrs.	θ

TABLE I (*Contd.*)

No.	Composition atomic %		Thermal analysis arrests (° C.)	Heat treatment				X-ray analysis results
				Regulus		Powder		
	Mn	Ga		Temperature (° C.)	Time	Temperature (° C.)	Time	
16	45	55	802; 773 724; 624	720	50 hrs.	750	90 min. (incipient melting)	η
				700	60 hrs.	700	4 hrs.	θ
						300	20 hrs.	θ
				620	40 hrs.			$\theta + Mn_5Ga_7$
						720	3 hrs. (incipient melting)	θ
						620	1 hr.	$\theta + Mn_5Ga_7$
				580	40 hrs.			$\theta + Mn_5Ga_7$
				520	40 hrs.			θ
						520	1 hr.	θ
17	42·5	57·5		as-cast				$\theta + Mn_5Ga_7 + MnGa_4$
				700	60 hrs.	700	20 hrs. (incipient melting)	$\theta + MnGa_4$
				600	40 hrs.	620	1 hr.	$\theta + Mn_5Ga_7$
						300	1 hr.	$\theta + Mn_5Ga_7$
18	42	58		560	60 hrs.	560	1 hr.	Mn_5Ga_7
19	41	59		560	60 hrs.	560	1 hr.	$Mn_5Ga_7 + Mn_3Ga_5$
20	40	60	756; 721 624; 604 547; 515	as-cast				$\eta + \theta + MnGa_4$
				700	40 hrs. (incipient melting)			$\theta + MnGa_4$
				620	40 hrs.			$Mn_5Ga_7 + MnGa_4$
				600	40 hrs.	620	1 hr.	$Mn_5Ga_7 + MnGa_4$
						600	1 hr.	$Mn_5Ga_7 + Mn_3Ga_5$
						300	1 hr.	$Mn_5Ga_7 + Mn_3Ga_5$

	21	37·5	62·5			as-cast			$\theta + Mn_2Ga_5 + MnGa_4$
						600	40 hrs.	620	1 hr. $\theta + Mn_5Ga_7 + MnGa_4$ (incipient melting)
								610	1 hr. $Mn_3Ga_5 + MnGa_4$ (incipient melting)
								600	1 hr. Mn_3Ga_5
								300	1 hr. Mn_3Ga_5
	22	35	65	720; 623		as-cast			$\theta + Mn_5Ga_7 + MnGa_4$
				603; 547		700	40 hrs.		$Mn_5Ga_7 + MnGa_4$
				517; 495		(incipient melting)			
				337		620	40 hrs.	620	1 hr. $Mn_5Ga_7 + MnGa_4$
						580	40 hrs.	580	1 hr. $Mn_3Ga_5 + MnGa_4$
						520	40 hrs.	400	1 hr. $Mn_3Ga_5 + Mn_2Ga_5$
	23	33	67			as-cast		500	24 hrs. $Mn_3Ga_5 + MnGa_4$
								300	48 hrs. $Mn_3Ga_5 + Mn_2Ga_5 + MnGa_4$
						powder pressed			
						+450	120 hrs.		$Mn_3Ga_5 + Mn_2Ga_5$
						powder pressed			
						+400	150 hrs.		$Mn_3Ga_5 + Mn_2Ga_5$
								550	12 hrs. $Mn_3Ga_5 + MnGa_4$
								490	12 hrs. $Mn_3Ga_5 + Mn_2Ga_5$
								400	4 hrs. $Mn_3Ga_5 + Mn_2Ga_5$
	24	31	69			450	70 hrs.	450	70 hrs. $Mn_3Ga_5 + Mn_2Ga_5 + MnGa_4$
						powder pressed			
						+400	150 hrs.	510	4 hrs. $Mn_3Ga_5 + Mn_2Ga_5 + MnGa_4$
								500	4 hrs. $Mn_3Ga_5 + Mn_2Ga_5$
								400	4 hrs. $Mn_3Ga_5 + Mn_2Ga_5$
	25	30	70	683; 617		as-cast			$Mn_3Ga_5 + MnGa_4 + Ga$
				600: 545					
				513; 494		600	70 hrs.	600	1 hr. $Mn_3Ga_5 + MnGa_4$
				323		powder pressed			
						+400	150 hrs.		$Mn_3Ga_5 + Mn_2Ga_5$
								510	12 hrs. $Mn_3Ga_5 + MnGa_4$
								480	12 hrs. $Mn_3Ga_5 + Mn_2Ga_5$
								400	4 hrs. $Mn_3Ga_5 + Mn_2Ga_5$

TABLE I (*Contd.*)

No.	Composition atomic %		Thermal analysis arrests (° C.)	Heat treatment				X-ray analysis results
				Regulus		Powder		
	Mn	Ga		Temperature (° C.)	Time	Temperature (° C.)	Time	
26	29	71		450	20 hrs.			Mn_3Ga_5 + Mn_2Ga_5 + $MnGa_4$
				powder pressed +460	150 hrs.			Mn_2Ga_5
						450	4 hrs.	Mn_2Ga_5
						175	40 hrs.	Mn_2Ga_5
27	27	73		450	20 hrs.			Mn_2Ga_5 + $MnGa_4$
				powder pressed +460	150 hrs.	450		Mn_2Ga_5 + $MnGa_4$
28	25	75	645; 543 518; 490 (373); 315	as-cast				Mn_2Ga_5 + $MnGa_4$ + Ga
				550	500 hrs. (incipient melting)	550	7 hrs.	Mn_3Ga_5 + $MnGa_4$ + Ga
						300	110 days	Mn_2Ga_5 + $MnGa_4$
				510	500 hrs. (incipient melting)			Mn_3Ga_5 + $MnGa_4$ + Ga
						200	10 hrs.	Mn_2Ga_5 + $MnGa_4$
				450	500 hrs.			Mn_2Ga_5 + $MnGa_4$
29	20	80	623; 516 495; 308	450	500 hrs.			$MnGa_4$
						200	10 hrs.	$MnGa_4$

30	18	82			250	50 hrs.		$MnGa_4 + MnGa_6$
							360 4 hrs.	$MnGa_4 + MnGa_6$
							340 4 hrs.	$MnGa_4 + MnGa_6$
							300 4 hrs.	$MnGa_4 + MnGa_6$
							250 4 hrs.	$MnGa_4 + MnGa_6$
					powder pressed			
					+370	70 hrs.		$MnGa_4 + Ga$
					powder pressed			
					+340	70 hrs.		$MnGa_4 + MnGa_6$
31	16	84			380	20 hrs.		$MnGa_4 + MnGa_6$
					powder pressed			
					+360	40 hrs.		$MnGa_4$
					powder pressed			
					+340	70 hrs.		$MnGa_6$
							300 40 hrs.	$MnGa_4 + MnGa_6$
32	15	85	591; 517 495; 312		340	50 hrs.		$MnGa_4 + MnGa_6$
33	14	86			as-cast			$Mn_2Ga_5 +$ $MnGa_4 + MnGa_6$
					360	40 hrs.		$MnGa_4$
					300	40 hrs.		$MnGa_6$
34	12	88			as-cast			$MnGa_4$
					360	40 hrs.		$MnGa_4$
					300	40 hrs.		$MnGa_6$
35	10	90	556; 518 494		as cast			Mn_2Ga_5+ $MnGa_4 + Ga$
					300	60 hrs.		$MnGa_6 +$ Melt

TABLE II

Analysis of the structure of the η phase in the manganese-gallium system

Alloy: $Mn_{54}Ga_{46}$ cooled in the furnace from the melt.
Radiation: CuK_α.
Structure: Cr_5Al_8 type, C_{3v}^5-R3 m; $a_r = 9{,}02_8$ Å, $\alpha = 88°\,24'$; $a_h = 12{,}58_7$ Å, $c_h = 16{,}07_0$ Å
Remarks: The reflections which do not fulfil the conditions $(h - k + l)_h = 3\,n$ and $(h + k + l)_r = 2\,n$ are omitted.

$(hkl)_r$	$(hkl)_h$	$10^3 . \sin^2\theta$		Observed intensity		
		Calculated	Observed	(Mn_7Ga_8)	(Cr_5Al_8)	
				Authors	Authors	Bradley and Lu
(110)	(102)	14·21	..	not obs.	vw	..
(01$\bar{1}$)	(110)	15·00	15·00	vvw	w	m
(020)	(022)	29·21	..	not obs.	not obs.	..
(121)	(014)	41·82	..	not obs.	vvw	..
(12$\bar{1}$)	(212)	44·21	..	not obs.	mw	w
(11$\bar{2}$)	(300)	45·05	..	not obs.	mw	..
(220)	(204)	56·82	56·90	vw	vw	..
(02$\bar{2}$)	(220)	60·01	..	not obs.	not obs.	..
(130)	(124)	71·82	71·78	vvw	not obs.	..
(03$\bar{1}$)	(132)	74·22	74·23	vw	not obs.	..
(222)	(006)	82·84	82·87	vw	vw	vvw
(22$\bar{2}$)	(402)	89·22	89·23	mw	w–	vw
(231)	(116)	97·84	97·55	vw	vvw	..
(23$\bar{1}$)	(314)	101·83	101·74	vvw	not obs.	..
(13$\bar{2}$)	(322)	104·22	104·39	vvw	not obs.	..
($\bar{1}$3$\bar{2}$)	(140)	105·02	105·13	vvw	vw	..
(040)	(044)	116·83	..	not obs.	not obs.	..
(330)	(306)	127·85	127·84	vs	s	vs
(141)	(036)					
(14$\bar{1}$)	(234)	131·84	131·83	vs	ms	
($\bar{1}$4$\bar{1}$)	(052)	134·23	134·28	s	s	
(03$\bar{3}$)	(330)	135·02	135·12	s		
(240)	(226)	142·85	142·53	vvw	not obs.	..
(04$\bar{2}$)	(242)	149·23	148·60	vvw	not obs.	..
(332)	(108)	152·27	152·05	vvw	vw	84
(33$\bar{2}$)	(504)	161·84	161·95	vw	w	127
(23$\bar{3}$)	(512)	164·24	164·13	s	w	291
(242)	(028)	167·27	167·78	vw	w	203
(24$\bar{2}$)	(424)	176·84	176·62	vw	w–	187
(22$\bar{4}$)	(600)	180·04	179·95	vvw	vvw	70
(341)	(218)	182·30	182·63	vvw	not obs.	18
(34$\bar{1}$)	(416)	187·86	187·79	w	vw	130
(150)	(146)					
(05$\bar{1}$)	(154)	191·85	191·48	vvw	vvw	25
(14$\bar{3}$)	(432)	194·24	194·24	vvw		65
(13$\bar{4}$)	(520)	195·04	..	not obs.	not obs.	11
(251)	(138)	212·28	212·65	vvw	not obs.	..
(25$\bar{1}$)	(336)	217·86	217·95	vvw	not obs.	..

TABLE II (*Contd.*)

$(hkl)_r$	$(hkl)_h$	$10^3.\sin^2\theta$		Observed intensity		
		Calculated	Observed (Mn_7/Ga_6) Authors		(Cr_5Al_8)	
					Authors	Bradley and Lu
$(15\bar{2})$	(344)	221·85	..	not obs.	not obs.	..
$(\bar{1}5\bar{2})$	(162)	224·25	..	not obs.	not obs.	..
(440)	(408)	227·34	..	not obs.	not obs.	..
$(34\bar{3})$	(01·10)	235·10	234·74	vvw	not obs.	..
$(04\bar{4})$	(440)	240·05	..	not obs.	not obs.	..
(350)	(328)	242·28	..	not obs.	not obs.	..
(442)	(20·10)	250·10	250·60	vw	vvw	obs.
$(34\bar{3})$	(614)	251·86			not obs.	
$(05\bar{3})$	(352)	254·25	..	not obs.	not obs.	..
$(33\bar{4})$	(702)					
$(44\bar{2})$	(606)	262·87	262·96	mw	w	obs.
(060)	(066)					
(352)	(12·10)	265·11	..	not obs.	vvw	obs.
$(42\bar{4})$	(622)	269·25	269·10	vw	w–	obs.
(161)	(058)	272·29	272·70	vw	not obs.	..
$(16\bar{1})$	(256)	277·88	277·68	vw	vvw	obs.
$(35\bar{2})$	(526)					
$(25\bar{3})$	(534)	281·87	..	not obs.	not obs.	..
$(\bar{1}6\bar{1})$	(074)					
$(23\bar{5})$	(710)	285·06	285·11	vvw	not obs.	..
(260)	(248)	287·29	..	not obs.	not obs.	..
(451)	(31·10)	295·01	..	not obs.	not obs.	..
$(06\bar{2})$	(264)	296·87	..	not obs.	not obs.	..
$(45\bar{1})$	(518)	302·30	..	not obs.	not obs.	..
$(26\bar{2})$	(04·10)	310·12	..	not obs.	not obs.	..
$(15\bar{4})$	(542)	314·26	..	not obs.	not obs.	..
$(14\bar{5})$	(630)	315·06	315·12	vw	not obs.	..
$(26\bar{2})$	(446)	322·88	323·74	vvw	not obs.	..
$(36\bar{1})$	(23·10)	325·12	..	not obs.	vvw	76
$(\bar{2}6\bar{2})$	(082)	329·26	..	not obs.	not obs.	..
(444)	(00·12)	331·34	..	not obs.	vw	81
$(36\bar{1})$	(438)	332·30	..	not obs.	not obs.	..
$(16\bar{3})$	(454)	341·88	341·35	w	mw	172
$(\bar{1}6\bar{3})$	$(27\bar{2})$	344·27	343·49	w		132
(453)	(11·12)	346·36	..	not obs.	vvw	38
(550)	(50·10)	355·13	..	not obs.	vw	101
$(44\bar{4})$	(804)	356·86	356·83	mw	mw	516
(170)	(168)	362·31	..	not obs.	not obs.	not obs.
$(45\bar{3})$	(716)	367·89	..	not obs.	not obs.	not obs.
$(07\bar{1})$	(176)					
(460)	(42·10)	370·12	370·59	vw	vvw	87
$(34\bar{5})$	(812)	374·28	..	not obs.	not obs.	not obs.
$(05\bar{5})$	(550)	375·08	376·39	m	w	470
(552)	(30·12)	376·39				
(363)	(03·12)				mw	729

TABLE III

Analysis of the structure of Mn_2Ga_5

Alloy: $Mn_{29}Ga_{71}$; pressed and sintered 150 hours at 460° C., powder 4 hours 450° C.
Radiation: CuK_α.
Structure: Mn_2Hg_5 type, D_{4h}^5-P_4/mbm; $a = 8{\cdot}80_3$ Å, $c = 2{,}69_4$ Å, $c/a = 0{\cdot}30_6$.
Remarks: The observed structure factors are compared with the observed structure factors of the zone (*hk*0) of Mn_2HG_5 (de Wet, 1961). Only the reflections not extinguished in the space group have been included.

(*hkl*)	$10^3.\sin^2\theta$		$F_{observed}$	
	Calculated	Observed	(Mn_2Ga_5)	(Mn_2Hg_5)
(110)	15·250	15·28	35	<14
(200)	30·500	30·45	42	50
(210)	38·125	38·21	75	63
(220)	61·000	61·01	98	141
(310)	76·250	76·21	242	208
(001)	81·420	81·38	530	..
(111)	96·670	96·52	42	..
(320)	99·125	99·11	239	208
(201)	111·920	111·98	250	..
(211)	119·545	119·51	250	..
(400)	122·000	121·95	126	182
(410)	129·625	129·46	433	341
(330)	137·250	137·17	365	294
(221)	142·420	142·46	224	..
(420)	152·500	152·67	317	180
(311)	157·670	157·59	228	..
(321)	180·545	180·28	204	..
(430)	190·625	190·80	53	<22
(510)	198·250	199·09	38	47
(401)	203·420	203·29	218	..
(411)	211·045	210·69	128	..
(331)	218·670	..	not obs.	..
(520)	221·125	..	not obs.	59
(421)	233·920	233·75	158	..
(440)	244·000	..	not obs.	96
(530)	259·250	258·93	185	80
(431)	272·045	271·06	48	..
(600)	274·500	275·53	97	<28
(511)	279·670	279·45	112	..
(610)	282·125	..	not obs.	<28
(521)	302·545	302·03	158	..
(620)	305·000	305·43	223	186
(540)	312·625	..	not obs.	149
(441)	325·420	325·48	316	..
(002)	325·680		633	..

TABLE III (*Contd.*)

(*hkl*)	$10^3.\sin^2\theta$		$F_{observed}$	
	Calculated	Observed	(Mn_2Ga_5)	(Mn_2Hg_5)
(531)	340·670	..	not obs.	..
(112)	340·930	..	not obs.	..
(630)	343·125	343·00	224	200
(601)	355·920	355·48	79	..
(202)	356·180		79	..
(611)	363·545	363·02	56	..
(212)	363·805		56	..
(710)	381·250	380·73	331	202
(550)			468	206
(621)	386·420	386·16	234	..
(222)	386·680		331	..
(541)	394·065	393·92	177	..
(640)	396·500	..	not obs.	<28
(312)	401·930	402·46	68	..
(720)	404·125	..	not obs.	<28
(631)	424·545	424·66	250	..
(322)	424·705		250	..
(730)	442·250	..	not obs.	<28
(402)	447·680	..	not obs.	..
(412)	455·305	454·90	250	..
(711)	462·670	462·31	353	..
(551)			250	..
(332)	462·930		353	..

Alloys containing more than 65 atomic % gallium exhibited sudden and striking volume changes on cooling in the vicinity of 500° C., as described earlier, and had often to be pressed for the heat treatments preceding the X-ray examination. This phenomenal increase in volume could be attributed to the peritectic formation at about 510° C. of the body-centered cubic $MnGa_4$ phase ($a = 5{\cdot}59_1$ Å), isostructural with $NiHg_4$, first examined by Lihl and Nowotny (1953). The diffraction data for $MnGa_6$ are set out in Table IV.

The orthorhombic C-face-centered $MnGa_6$ phase ($a = 8{\cdot}94_9$ Å, $b = 8{\cdot}81_4$ Å and $c = 9{\cdot}94_4$ Å) also forms peritectically at about 340° C. and exists in equilibrium with $MnGa_4$ on one side and with gallium itself on the other side. The powder reflections (Table V) point to the space group either C_{2v}^{13}-Ccc2 or D_{2h}^{20}-Cccm.

TABLE IV

Analysis of the structure of $MnGa_4$

Alloy: $Mn_{20}Ga_{80}$; regulus 500 hours at 450° C., powder 10 hours at 200° C.
Radiation: CuK_α.
Structure: $NiHg_4$ type, 0^5-I432; $a = 5{\cdot}59_1$ Å.
Remarks: Only those reflections not extinguished in the space group have been included.

(*hkl*)	$10^3.\sin^2\theta$		Intensity	
	Calculated	Observed	Calculated	Observed
(110)	38·02	38·06	116	m
(200)	76·04	76·07	469	vs
(211)	114·06	114·07	98	mw
(220)	152·08	152·05	990	vvs
(310)	190·10	190·07	43	w
(222)	228·12	228·12	204	s
(321)	266·14	266·04	61	w
(400)	304·16	304·15	270	s
(330)	342·18	342·18	12	w
(411)			24	
(420)	380·20	380·40	326	s
(332)	418·22	418·34	14	vw

4. DISCUSSION OF RESULTS

The manganese-gallium system has proved to be a complex and interesting one with not less than ten intermediate phases besides gallium and the four terminal solid solutions in manganese. Eight peritectic reactions, five solid-state reactions and one simple phase transformation in the solid state have been established in alloys of this system with reasonable certainty. Evidence for two more phase transformations (Table VII, Nos. 4 and 12) has been obtained, but needs further detailed experimental confirmation. While gallium is capable of dissolving in solid manganese to an extent of over 25

TABLE V

Analysis of the structure of $MnGa_6$

Alloy: $Mn_{12}Ga_{88}$; 40 hours at 300° C.

Radiation: CuK_α.

Structure: Not completely resolved; either C_{2v}^{13}-Ccc2 or D_{2h}^{20}-Cccm; $a = 8{\cdot}94_9$ Å, $b = 8{\cdot}81_4$ Å, $c = 9{\cdot}94_4$ Å.

Remarks: Only those reflections not extinguished in the space group have been included.

(*hkl*)	$10^3 . \sin^2\theta$		Intensity observed
	Calculated	Observed	
(110)	15·07	..	not obs.
(111)	21·08	21·09	m
(002)	24·04	..	not obs.
(200)	29·68	29·68	m
(020)	30·60	30·63	m
(112)	39·11	..	not obs.
(202)	53·72	53·71	m
(022)	54·64	54·66	m
(220)	60·28	60·26	w
(221)	66·29	..	not obs.
(113)	69·16	69·27	vw
(310)	74·43	74·32	vw
(130)	76·27	76·34	w
(311)	80·44	80·38	s
(131)	82·28	82·29	w
(222)	84·32	84·32	vs
(004)	96·16	96·52	s
(312)	98·47	98·49	m
(132)	100·31	100·26	m
(114)	111·23	111·43	vw
(223)	114·37	..	not obs.
(400)	118·72	118·67	s
(040)	122·40	122·07	m
(204)	125·84	126·10	s
(024)	126·76	126·91	w
(313)	128·52	128·55	s
(133)	130·36	130·77	s
(330)	135·63	134·20	vw
(331)	141·64	141·42	s
(402)	142·76	142·88	s
(042)	146·44	146·20	s
(420)	149·32	149·30	m
(240)	152·08	152·29	w
(421)	155·33	155·06	w
(224)	156·44	156·71	s

TABLE V (*Contd.*)

(*hkl*)	$10^3.\sin^2\theta$		Intensity observed
	Calculated	Observed	
(241)	158·09	157·98	vw
(332)	159·67	160·27	w
(115)	165·32	165·82	m
(314)	170·59	170·40	vw
(134)	172·43	172·50	vw
(422)	173·36	172·96	vvw
(242)	176·12	176·08	m
(333)	189·72	189·70	w
(510)	193·15	193·27	mw
(150)	198·67	198·68	vw
(511)	199·16		
(423)	203·42	203·71	w
(151)	204·68		
(243)	206·17	206·25	w
(225)	210·53	..	not obs.
(404)	214·88	214·94	vw
(006)	216·36	216·94	vw
(512)	217·19		
(044)	218·56	..	not obs.
(152)	222·71	..	not obs.
(315)	224·68	..	not obs.
(135)	226·52	226·22	vw
(116)	231·43	..	not obs.
(334)	231·79	..	not obs.
(440)	241·12	240·84	s
(424)	245·48	..	not obs.
(206)	246·04	246·98	vvw
(026)	246·96		
(441)	247·13		
(244)	248·24	248·49	vw
(530)	254·35	254·55	vw
(350)	258·03	257·60	vw
(531)	260·36	..	not obs.
(351)	264·04	264·34	w
(442)	265·16		
(600)	267·12	266·81	w
(060)	275·40	274·72	w
(226)	276·64	277·37	m
(532)	278·39		
(352)	282·07	..	not obs.
(335)	285·88	286·16	m
(514)	289·31	..	not obs.
(316)	290·79	290·59	w
(602)	291·16		

TABLE V (*Contd.*)

(*hkl*)	$10^3 . \sin^2\theta$		Intensity observed
	Calculated	Observed	
(136)	292·63	292·34	vvw
(154)	294·83	..	not obs.
(443)	295·21	..	not obs.
(620)	297·72	..	not obs.
(062)	299·44	298·87	vvw
(425)	299·57		
(245)	302·33	303·51	w
(621)	303·73		
(260)	305·08	..	not obs.
(533)	308·44	309·14	vw
(117)	309·56		
(261)	311·09	310·76	m
(353)	312·12	..	not obs.
(603)	321·21	321·31	w
(622)	321·76		
(262)	329·12	328·65	vw
(063)	329·49		
(406)	335·08	335·40	
(444)	337·28	..	w
(046)	338·76	339·37	
(515)	343·40	..	not obs.
(155)	348·92	..	not obs.
(534)	350·51		
(623)	351·81	351·31	m
(336)	351·99		
(227)	354·77	..	not obs.
(263)	359·17	359·32	vw
(604)	363·28	363·36	vw
(426)	365·68	..	not obs.
(246)	368·44	..	not obs.
(317)	368·92	370·09	
(137)	370·76	..	vw
(710)	371·23	..	
(064)	371·56	371·44	
(550)	376·75	..	not obs.
(711)	377·24	..	not obs.
(170)	382·27	382·61	w
(551)	382·76		
(008)	384·64	..	not obs.
(171)	388·28	386·94	w
(640)	389·52	389·40	w
(445)	391·37	..	not obs.

TABLE V (*Contd.*)

(*hkl*)	$10^3.\sin^2\theta$		Intensity observed
	Calculated	Observed	
(624)	393·88	394·34	s
(460)	394·12	..	
(712)	395·27	..	
(641)	395·53	395·19	
(118)	399·71	401·00	m
(461)	400·13	..	
(552)	400·79	..	
(264)	401·24	402·54	
(535)	404·60	..	not obs.
(172)	406·31	..	not obs.
(355)	408·28	..	not obs.
(516)	409·51	..	not obs.
(642)	413·56	..	not obs.
(208)	414·32	..	not obs.
(156)	415·03	..	not obs.
(028)	415·24	..	not obs.
(462)	418·16	418·67	vw
(713)	425·32	..	not obs.
(337)	430·12	..	not obs.
(553)	430·84	431·97	w
(730)	432·43		
(173)	436·36	..	not obs.

atomic %, manganese does not seem to have any solubility in solid gallium. Five intermetallic compounds with small ranges of homogeneity are formed, all on the gallium-rich side of the system.

The manganese-rich portion of this system displays a striking similarity to the manganese-zinc system in the formation at higher temperatures of the extensive A1 solid solution and the A3 and γ-brass type phases with increasing gallium content. It can be concluded from this tendency that one electron per Mn-atom develops a brass-type bonding with the three valency electrons of gallium. At lower temperatures, correlations (couplings) between the electrons of the outermost shell of manganese are set up, leading to the complex θ, Mn_5Ga_7 and Mn_3Ga_5 phases as also to the simpler ζ_1 and ζ_2 phases.

An interesting phase of the system is the η phase, with the gradual rhombohedral distortion of its structure from the Mn_8Ga_5 to the Mn_7Ga_6

TABLE VI

Crystal structures in the manganese-gallium system

No.	Phase	Structure type	Typical composition	Lattice parameters	References
1	α-Mn	α-Mn	..	$a = 8{\cdot}912$ Å	Hansen and Anderko (1958)
2	β-Mn	β-Mn	$Mn_{85}Ga_{15}$	$a = 6{\cdot}37_5$ Å	Zwicker (1951) measurement : this paper
3	γ-Mn	Cu	$Mn_{75}Ga_{25}$	$a = 3{\cdot}76_9$ Å	Measurement : this paper
4	γ-Mn (*t*)	CuAu I	$Mn_{85}Ga_{15}$	$a = 3{\cdot}79_0$ Å $c/a = 0{\cdot}96_8$	do.
5	δ-Mn	W	..	$a = 3{\cdot}080$ Å	Hansen and Anderko (1958)
6	ε	Mg	$Mn_{70}Ga_{30}$	$a = 2{\cdot}67_8$ Å $c/a = 1{\cdot}62_0$	Zwicker (1951) measurement : this paper
7	ζ_1	CuAu I	,,	$a = 3{\cdot}89_8$ Å $c/a = 0{\cdot}92_0$	do.
8	ζ_2	,,	$Mn_{55{\cdot}5}Ga_{44{\cdot}5}$	$a = 3{\cdot}88_4$ Å $c/a = 0{\cdot}95_2$	This paper
9	η	Cr_5Al_8	$Mn_{54}Ga_{46}$	$a_r = 9{\cdot}02_8$ Å $\alpha = 88°24'$	Schubert *et al.* (1960)
10	θ	Unknown	$Mn_{47{\cdot}5}Ga_{52{\cdot}5}$	..	..
11	Mn_5Ga_7	,,	$Mn_{42}Ga_{58}$	..	..
12	Mn_3Ga_5	,,	$Mn_{37{\cdot}5}Ga_{62{\cdot}5}$	..	..
13	Mn_2Ga_5	Mn_2Hg_5	$Mn_{29}Ga_{71}$	$a = 8{\cdot}80_3$ Å $c/a = 0{\cdot}39_6$	Schubert *et al.* (1962)
14	$MnGa_4$	$NiHg_4$	$Mn_{20}Ga_{80}$	$a = 5{\cdot}59_1$ Å	do. (1960)
15	$MnGa_6$	Orthorhombic	$Mn_{14}Ga_{86}$	$a = 8{\cdot}94_9$ Å $b = 8{\cdot}81_4$ Å $c = 9{\cdot}94_4$ Å	This paper
16	Ga	Ga	..	$a = 4{\cdot}526$ Å $b = 4{\cdot}520$ Å $c = 7{\cdot}660$ Å	Hansen and Anderko (1958)

composition, and with its decomposition on cooling either to the ζ_2 phase or the θ phase or to both eutectoidally at different compositions. Its formula Mn_8Ga_5 on the manganese-rich side displays a close similarity with the γ-brass phases (*e.g.*, Cu_5Zn_8, Cr_5Al_8, Mn_5Al_8, etc.), although its structure is not body-centered like γ-brass. Actually, a study of the variation of mean atomic volume with gallium content reveals better agreement for 53 atoms in the unit cell than for 52 atoms characteristic of γ-brass (Text-Fig. 3). The formula $Mn_{32}Ga_{21}$ (*i.e.*, $Mn_8Ga_{5{\cdot}25}$) also agrees better than Mn_8Ga_5 with the observed

TABLE VII

Reactions in the manganese-gallium system

No.	Temperature (° C.)	Type	Details
1	1180	Peritectic	$\delta + L \rightleftharpoons \gamma$
2	990	Peritectic	$\gamma + L \rightleftharpoons \epsilon$
3	880	Peritectic	$\epsilon + L \rightleftharpoons \eta'$
4	860....770	Phase transformation	$\eta' \rightleftharpoons \eta$
5	750	Peritectoidal	$\epsilon + \eta \rightleftharpoons \zeta_1$
6	720	Peritectic	$\eta + L \rightleftharpoons \theta$
7	650	Eutectoidal	$\gamma \rightleftharpoons \beta + \epsilon$
8	650	Phase transformation	$\eta \rightleftharpoons \zeta_2$
9	620	Peritectic	$\theta + L \rightleftharpoons Mn_5Ga_7$
10	600	Peritectic	$Mn_5Ga_7 + L \rightleftharpoons Mn_3Ga_5$
11	560	Eutectoidal	$\eta \rightleftharpoons \zeta_2 + \theta$
12	545	Phase transformation	α-$Mn_5Ga_7 \rightleftharpoons \beta$-$Mn_5Ga_7$
13	530	Eutectoidal	$\epsilon \rightleftharpoons \beta + \zeta_1$
14	510	Peritectic	$Mn_3Ga_5 + L \rightleftharpoons MnGa_4$
15	490	Peritectoidal	$Mn_3Ga_5 + MnGa_4 \rightleftharpoons Mn_2Ga_5$
16	340	Peritectic	$MnGa_4 + L \rightleftharpoons MnGa_6$

composition limit of the η phase on the manganese side. The availability of an extra atom (here a gallium atom) also may explain the observed deviation from the body-centered structure. Non-body-centered γ-brass structures are known and are characterized, in cases of appreciable composition ranges of stability, by the development of vacant lattice sites and lattice distortions (Hume-Rothery *et al.*, 1951; Reynolds *et al.*, 1951). As shown in the case of Cu_9Ga_4, the number of atoms in the unit cell can go down from 52 to as low as 47 (Betterton *et al.*, 1951). The special feature of the η phase in the

manganese-gallium system is that its unit cell contains 53 atoms on the manganese side and moves over to the formula Mn_7Ga_6 (only 52 atoms) with rhombohedral distortion. Thus, on addition of gallium, *i.e.*, increase of electron concentration, the structure reacts by forming a vacant site, in addition to becoming distorted and unstable at lower temperatures.

Among the gallium-rich phases, the structures of only Mn_2Ga_5 and $MnGa_4$ have been resolved in the present work (Text-Fig. 4). The $MnGa_4$ structure is the simpler one of the two phases and has a structural counterpart in $NiHg_4$ and $PtHg_4$. As the valency electrons of the non-transition components (*i.e.*, Ga and Hg) of this structure have a tendency for an A2 correlation and as they also happen to be the predominant components, it is reasonable to assume that they determine the bonding characteristics in this structure. With $a/2 = a_{A2}$, 16 places are available in the cubic unit cell with electronic separations of 2·6 and 2·4 Å for mercury and gallium respectively. These values appear to be rather high in the light of the electronic separations in the elements themselves. The 16 places in the unit cell necessitate that only 2 electrons of each atom of the non-transition element can take part in correlation. This means that each manganese atom has to absorb 4 valency electrons, which is possible only when it is still in a position to build up its conduction band with one electron per atom. The A_2 correlation is further hinted at by the value of the mean atomic volume of $MnGa_4$, which is higher than expected.

The Mn_2Ga_5 structure is the same as that of Mn_2Hg_5 with alternate layers of atoms of the transition and non-transition elements respectively in the direction of the *c*-axis. The conclusion is inevitable that $a/\sqrt{10} = a_{A2}$, so that two electronic-site layers are available for every *c*-axis and that there are 10 places for each formula unit. Every manganese atom has to absorb 2·5 electrons, *i.e.*, there is room for a magnetic moment. In point of fact, Mn_2Ga_5 has been found to be ferromagnetic.

5. Summary

The constitution of manganese-gallium alloys has been investigated, chiefly by thermal analysis and X-ray methods. The binary phase diagram has been established, displaying eight peritectic, three eutectoidal and two peritectoidal reactions. Ten intermediate phases have been recognized and the structures of six of them have been resolved. The details of the constitutional diagram have been discussed in relation to allied systems and in the light of the valency electron interactions.

6. ACKNOWLEDGEMENT

It is a pleasure for the authors to express their deep sense of gratitude to Prof. Dr. Werner Koester, Director, Max-Planck-Institut fuer Metallforschung, for his interest in the present work. One of the authors (T. R. A.) is indebted to the Max-Planck-Institut fuer Metallforschung and the Stuttgart Technische Hochschule for financial assistance during the course of the present investigations.

7. REFERENCES

Betterton, J. O. and Hume-Rothery, W. — *J. Inst. Met.*, 1951, **80**, 459.

Bradley, A. J. and Lu, S. S. .. — *Ibid.*, 1937, **60**, 319; *Z. Krist.*, 1937, **96**, 20.

Hansen, M. and Anderko, K. .. — *Constitution of Binary Alloys*, McGraw-Hill Book Company, Inc., New York, Toronto, London, 1958, p. 1266.

Hume-Rothery, W., Betterton, J. O. and Reynolds, J. — *J. Inst. Met.*, 1951, **80**, 609.

Koester, W. and Wachtel, E. .. — *Z. Metallkunde*, 1960, **51**, 271.

Lihl, F. and Nowotny, H. .. — *Ibid.*, 1953, **44**, 359.

Schubert, K., Anantharaman, T. R., Ata, H. O. K., Meissner, H. G., Poetzschke, M., Rossteutscher, W. and Stolz, E. — *Naturwiss.*, 1960, **47**, 512.

———, Meissner, H. G., Poetzschke, M., Rossteutscher, W. and Stolz, E. — *Ibid.*, 1962, **49**, 57.

Thiele, W. and Zwicker, U. — In *Constitution of Binary Alloys* by M. Hansen and K. Anderko, McGraw-Hill Book Company,. Inc., New York, Toronto, London, 1958, p. 748.

de Wet, J. F. .. — *Acta Cryst.*, 1961, **14**, 733.

Zwicker, U. .. — *Z. Metallkunde*, 1951, **42**, 248, 329.

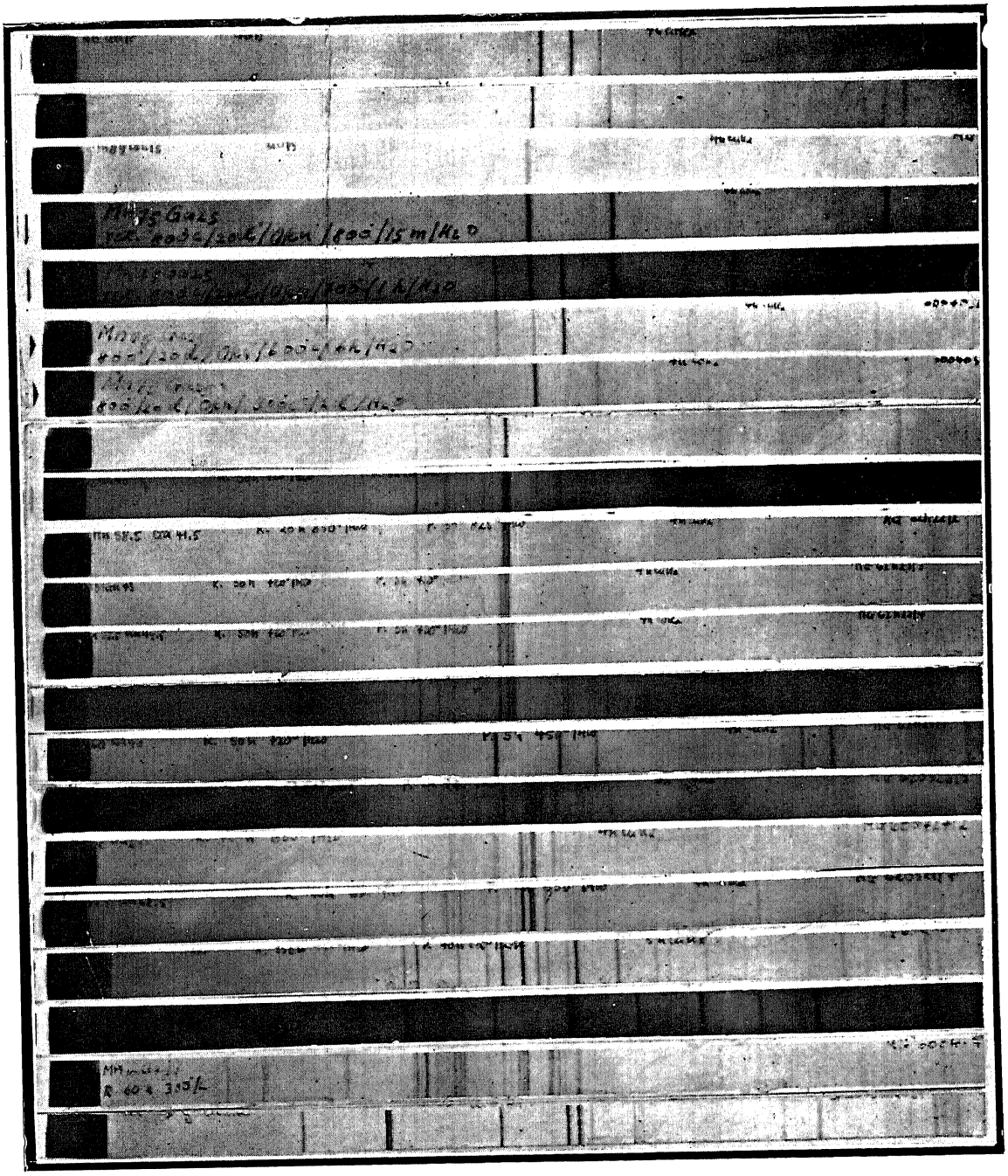

FIG. 1

EXPLANATION OF PLATE XVI

FIG. 1. Guinier patterns of different phases of the manganese-gallium system (CuKα Radiation).

No.	Phase	Composition	Temperature
1	β-Mn	$Mn_{90}Ga_{10}$	as cast
2	γ-Mn (t)	$Mn_{90}Ga_{10}$	1000° C.
3	γ-Mn	$Mn_{85}Ga_{15}$	as cast
4	γ-Mn	$Mn_{75}Ga_{25}$	800° C.
5	γ-Mn + ϵ	$Mn_{75}Ga_{25}$	700° C.
6	ϵ	$Mn_{75}Ga_{25}$	600° C.
7	ζ_1	$Mn_{75}Ga_{25}$	300° C.
8	$\zeta_1 + \eta$	$Mn_{62.5}Ga_{37.5}$	720° C.
9	η	$Mn_{60}Ga_{40}$	720° C.
10	η	$Mn_{58.5}Ga_{41.5}$	825° C.
11	η	$Mn_{57}Ga_{43}$	720° C.
12	η	$Mn_{55.5}Ga_{44.5}$	720° C.
13	η	$Mn_{55}Ga_{45}$	720° C.
14	ζ_2	$Mn_{60}Ga_{40}$	450° C.
15	θ	$Mn_{47.5}Ga_{52.5}$	700° C.
16	$Mn_5Ga_7 + Mn_3Ga_5$	$Mn_{40}Ga_{60}$	600° C.
17	Mn_3Ga_5	$Mn_{37.5}Ga_{62.5}$	550° C.
18	Mn_2Ga_5	$Mn_{29}Ga_{71}$	175° C.
19	$MnGa_4$	$Mn_{20}Ga_{80}$	450° C.
20	$MnGa_6$	$Mn_{10}Ga_{90}$	300° C.
21	Ga	..	..